Eliminating leading corrections to scaling in the three-dimensional $O(N)$-symmetric ϕ^4 model: $N = 3$ and 4

2001 J. Phys. A: Math. Gen. 34 8221

(http://iopscience.iop.org/0305-4470/34/40/302)

INSTITUTE OF PHYSICS PUBLISHING JOURNAL OF PHYSICS A: MATHEMATICAL AND GENERAL

J. Phys. A: Math. Gen. **34** (2001) 8221–8236 PII: S0305-4470(01)18975-4

Eliminating leading corrections to scaling in the three-dimensional $O(N)$-symmetric ϕ^4 model: $N = 3$ and 4

Martin Hasenbusch[1]

Humboldt-Universität zu Berlin, Institut für Physik, Invalidenstrasse 110, D-10115 Berlin, Germany

E-mail: Martin.Hasenbusch@desy.de

Received 10 November 2000, in final form 26 June 2001
Published 28 September 2001
Online at stacks.iop.org/JPhysA/34/8221

Abstract

We study corrections to scaling in the $O(3)$- and $O(4)$-symmetric ϕ^4 model on the three-dimensional simple cubic lattice with nearest-neighbour interactions. For this purpose, we use Monte Carlo simulations in connection with a finite-size scaling method. We find that a finite value of the coupling λ^* exists for both values of N, where leading corrections to scaling vanish. As a first application, we compute the critical exponents $\nu = 0.710(2)$ and $\eta = 0.0380(10)$ for $N = 3$ and $\nu = 0.749(2)$ and $\eta = 0.0365(10)$ for $N = 4$.

PACS numbers: 05.10.Ln, 05.50.+q, 64.60.-i

1. Introduction

At a second-order phase transition various quantities diverge with power laws. For example, the magnetic susceptibility behaves as

$$\chi \sim C_{\pm} |t|^{-\gamma} \tag{1}$$

where $t = (T - T_c)/T_c$ is the reduced temperature. The subscripts + and − indicate the high- and low-temperature phases, respectively. γ is the critical exponent of the magnetic susceptibility.

The universality hypothesis says that for all systems within a given universality class the exponent γ, as other critical exponents, takes exactly the same value. Note that the amplitudes $C_{\pm}$ depend on the details of the system, while the ratio C_+/C_- is universal; i.e. it takes the same value for all systems within a universality class. A universality class is characterized by the spatial dimension of the system, the range of the interaction and the symmetry of the order parameter (see [1]).

[1] Present address: NIC/DESY Zeuthen Platanenallee 6, D-15738 Zeuthen, Germany.

Precise estimates of universal quantities, such as critical exponents and universal amplitude ratios, obtained for theoretical models and experimental systems, are needed to test the universality hypothesis.

One theoretical approach is the study of lattice spin models such as the Ising model. In three dimensions, where no exact solution of these models is available, the most precise results are obtained by the analysis of high-temperature series and Monte Carlo simulations. For universal quantities, a similar accuracy can be obtained with field-theoretic methods such as the ϵ-expansion or perturbation theory in three dimensions. For a detailed discussion see textbooks on critical phenomena; for example, [2, 3].

Here we consider universality classes, which are characterized by $O(N)$ symmetry and short-range interactions for the cases $N = 3$ (Heisenberg universality class) and $N = 4$.

For this purpose, we study $O(N)$-invariant ϕ^4 models on the simple cubic lattice. We consider periodic boundary conditions. Here, the lattices have the linear extension L in all three directions. The action is given by

$$S = -\beta \sum_{\langle xy \rangle} \vec{\phi}_x \cdot \vec{\phi}_y \;\; + \sum_x \vec{\phi}_x^2 \; + \; \lambda \sum_x (\vec{\phi}_x^2 - 1)^2 \tag{2}$$

where $\vec{\phi}_x \in \mathbb{R}^N$ and $\langle xy \rangle$ denotes a pair of nearest-neighbour sites on the lattice. The action is related to the classical Hamiltonian by $S = \beta H$, where $\beta = 1/k_B T$. We study the canonical ensemble; i.e. the partition function is given by

$$Z = \int \mathrm{D}[\phi] \;\; \exp(-S) \tag{3}$$

where $\int \mathrm{D}[\phi]$ is shorthand for the $N \times L^3$ dimensional integral over all components of the field at all lattice points. $\lambda = 0$ gives the exactly solvable Gaussian model. In the limit $\lambda = \infty$ the last term of the action forces the field to unit-length, $\vec{\phi}_x^2 = 1$; that is, the $O(N)$-invariant nonlinear σ models are recovered. The $O(3)$-invariant nonlinear σ model is also called the classical Heisenberg model. Along a critical line $\beta_c(\lambda)$, the model undergoes a second-order phase transition. For all $\lambda > 0$, at given N, these transitions belong to the same universality class.

In previous Monte Carlo studies of the Heisenberg [4–9] and the $O(4)$ [9–11] universality classes, $O(N)$-invariant nonlinear σ models have been studied. Mostly, the critical exponents ν and η have been computed by finite-size scaling. To this end, the models have been simulated at the critical temperature T_c for various system sizes L. For instance, the exponent η can then be obtained by fitting the data for the magnetic susceptibility with the ansatz

$$\chi|_{T_c} \sim c \; L^{2-\eta}. \tag{4}$$

The remaining exponents can then be inferred from scaling relations such as $2 - \eta = \gamma/\nu$.

While most of the results for the critical exponent ν of the correlation length are consistent with each other and with the results of field-theoretic methods, there is a clear discrepancy in the case of the exponent η. Most of the studies [5–8, 10, 11] have given $\eta < 0.03$ for $N = 3$ as well as $N = 4$. (A detailed discussion of the numbers will be given in section 6.) These results have to be compared, for example, with $\eta = 0.0375(45)$ for $N = 3$ and $\eta = 0.0360(40)$ obtained from the ϵ-expansion [12].

The authors of [9] have argued that this discrepancy is due to corrections to scaling that had been ignored in the analysis of the Monte Carlo data. In fact, taking into account leading corrections

$$\chi|_{T_c} = c \; L^{2-\eta} \; (1 \; + \; a L^{-\omega} + \cdots) \tag{5}$$

where $\omega \approx 0.8$, they found $\eta = 0.0413(16)$ for $N = 3$ and $\eta = 0.0384(12)$ for $N = 4$. Here, we try to clarify this situation and to corroborate the argument of [9]. However, we follow

a more radical strategy to deal with corrections $\propto L^{-\omega}$: we eliminate them. To this end, we make use of the parameter λ in the action (2). The critical exponents, including the correction exponent ω, are the same for all values of $\lambda > 0$. However, in equation (5), the correction amplitude a is a function of λ. Hence, there is a chance of finding a zero: $a(\lambda^*) = 0$. Note that renormalization group theory predicts that λ^* is unique for all quantities.

In [13, 14] a finite-size scaling method has been proposed that allows us to compute λ^* in a systematic way. This method has been successfully implemented for $N = 1$ (Ising universality class) [13–15] and $N = 2$ (XY universality class) [16, 17]. As a result, for these universality classes, the most precise estimates for critical exponents from Monte Carlo simulations have been obtained.

Furthermore, the results for λ^* obtained from Monte Carlo have been used as input for the analysis of high-temperature series [17–19]. As a result, the accuracy of the critical exponents was further improved and, in addition, a large set of universal amplitude combinations has been computed with unprecedented precision.

A priori, it is not clear whether this program can be extended to larger N. In fact, in [18] it was argued that for $N > 3$ no such λ^* exists for the action equation (2) on simple cubic lattices. The argument is based on the large N expansion and the analysis of high-temperature series expansions [20].

The paper is organized as follows. In section 2 we briefly review the finite-size scaling method to eliminate leading corrections to scaling. The Monte Carlo algorithm, which is a hybrid of the wall-cluster algorithm [14] and a local algorithm, is discussed in section 3. Details of the simulations are given in section 4. In section 5 we analyse our Monte Carlo data and give the results for λ^* and the critical exponents ν and η. A major goal of this study is to provide reliable error bars. Therefore, we discuss in detail how systematic errors due to leading and sub-leading corrections are estimated. Next we compare our results for the critical exponents with those given in the literature. Finally we give our conclusions.

2. The finite-size scaling method

2.1. Dimensionless ratios

Our method to locate λ^* can be viewed as a generalization of Nightingale's phenomenological renormalization group [21] or Binder's cumulant crossing method [22] to find β_c and to compute the renormalization group exponent $y_t = 1/\nu$. Therefore, we consider the same or similar dimensionless ratios as Nightingale and Binder [21, 22]. Dimensionless ratios are invariant under renormalization group transformations. The prototype of such a quantity is the so-called Binder cumulant:

$$U_4 = \frac{\langle(\vec{m}^2)^2\rangle}{\langle\vec{m}^2\rangle^2} \tag{6}$$

where

$$\vec{m} = \frac{1}{V}\sum_x \vec{\phi}_x \tag{7}$$

is the magnetization of the system. Note that higher moments of the magnetization could also be considered.

Frequently, the second moment correlation length divided by the linear extension of the lattice ξ_{2nd}/L has been studied. The second moment correlation length is defined by

$$\xi_{2nd} = \sqrt{\frac{\chi/F - 1}{4\,\sin(\pi/L)^2}} \tag{8}$$

where

$$\chi = \frac{1}{V}\left\langle \left(\sum_x \vec{\phi}_x \right)^2 \right\rangle \tag{9}$$

is the magnetic susceptibility and

$$F = \frac{1}{V}\left\langle \left| \sum_x \exp\left(\mathrm{i}\frac{2\pi x_1}{L} \right) \vec{\phi}_x \right|^2 \right\rangle \tag{10}$$

is the Fourier transform of the two-point correlation function at the lowest non-vanishing momentum. In order to reduce the statistical error, we averaged the results of all three directions of the lattice. Note that Nightingale [21] studied ξ/L, where ξ is the exponential correlation length of a system of the size $L^{D-1} \times \infty$.

The third quantity that we study is the ratio Z_a/Z_p of the partition function Z_a with anti-periodic boundary conditions in one of the three directions and Z_p with periodic boundary conditions in all directions. Anti-periodic boundary conditions mean that the term $\sum_{\langle xy \rangle} \vec{\phi}_x \cdot \vec{\phi}_y$ in the action is multiplied by -1 for $x = (L_1, x_2, x_3)$ and $y = (1, x_2, x_3)$. This ratio can be measured with the help of the boundary-flip algorithm, which is a version of the cluster algorithm. The boundary-flip algorithm was introduced in [23] for the Ising model. In [24] the authors have generalized this method to the case of $O(N)$-invariant nonlinear σ models. As in [15] we use a version of the algorithm that only measures Z_a/Z_p and does not perform the flip to anti-periodic boundary conditions. For a recent discussion of the algorithm see [17].

2.2. *Locating* λ^*

Below we shall briefly recall the theoretical basis of the finite-size scaling method that has been developed in [13–15] (see also [17]).

Let us denote a dimensionless ratio by R. We define a quantity $\bar{R}$ based on a pair of dimensionless ratios R_1 and R_2.

First we define β_f as the value of β where, at given λ and L, R_1 takes the fixed value $R_{1,f}$:

$$R_1(L, \lambda, \beta_f) = R_{1,f}. \tag{11}$$

Hence β_f is a function of L and λ. Note that in the language of high-energy physics, this is our 'renormalization condition'. Note that $\beta_f = \beta_c + \text{const}\, L^{-1/\nu} + \cdots$, where the constant depends on the choice of $R_{1,f}$.

Next we define

$$\bar{R}(L, \lambda) \equiv R_2(L, \lambda, \beta_f). \tag{12}$$

In the following we will frequently refer to $\bar{R}(L, \lambda)$ as 'R_2 at $R_{1,f}$'. The behaviour of $\bar{R}(L, \lambda)$ can be inferred from renormalization group theory (for a detailed derivation see [17]):

$$\bar{R}(L, \lambda) = \bar{R}^* + \bar{c}(\lambda)\, L^{-\omega} + \cdots. \tag{13}$$

In this equation, eliminating leading corrections to scaling means finding the zero of $\bar{c}(\lambda)$. One can imagine various numerical implementations to do this. Here we have followed the strategy used in [15, 16]. We have simulated the models close to the critical line for several values of λ for various lattice sizes. The results are then fitted by equation (13). The function $\bar{c}(\lambda)$ is then approximated by interpolation between the λ-values, where simulations have been performed. In the following, we always use either Z_a/Z_p or ξ_{2nd}/L as R_1 and U_4 as R_2. Note that in [15] we have only used $R_1 = Z_a/Z_p$ and in [16] only $R_1 = \xi_{2nd}/L$. Using both quantities gives us better control over systematic errors.

In order to estimate the systematic error of our result for λ^*, we need some knowledge of the corrections that are hidden in the $\cdots$ of equation (13). In addition to the term $\propto L^{-2\omega}$ there are sub-leading corrections with $\omega' > \omega$. While the value of $\omega \approx 0.8$ is well established (see, for example, [12]), unfortunately the knowledge of ω' is rather limited. Using the 'scaling field method', which is a version of Wilson's 'exact renormalization group', the authors of [25] have found $\omega_2 = 1.78(11)$ for $N = 3$. Following the figure given in [25] the value of ω_2 for $N = 4$ is similar to that of $N = 3$. In addition, there are corrections due to the breaking of the rotational invariance by the lattice. These corrections have an $\omega_{\text{rot}} \approx 2$ [26]. In the case of the Binder cumulant and the second moment correlation length, we have to expect corrections due to the analytic background of the magnetic susceptibility. This amounts to corrections with an exponent $\omega_{\text{back}} = 2 - \eta \approx 2$.

Since all ω' are larger than or equal to 2ω, we shall assume corrections $\propto L^{-1.6}$ when we estimate systematic errors.

3. The Monte Carlo algorithm

In the last decade it has been demonstrated that $O(N)$-invariant nonlinear σ models can be most efficiently simulated with cluster algorithms [28,29]. The advantage of cluster algorithms, compared with local algorithms such as the Metropolis algorithm, is that critical slowing down is almost completely eliminated. Hence, most of the recent Monte Carlo simulations of $O(N)$-invariant nonlinear σ models have been performed with a cluster algorithm. For example, the single-cluster algorithm [29] was used in the simulations [5–10] of the Heisenberg model and the $O(4)$-invariant nonlinear σ model in three dimensions.

In this study we have simulated the $O(N)$-invariant nonlinear σ models with the wall-cluster algorithm [14]. For finite λ, following Brower and Tamayo [27], additional updates with a local Metropolis algorithm were performed to allow fluctuations of the modulus of the field $\vec{\phi}_x$. Below, we give the details of the wall-cluster algorithm, the local update and the precise sequence of update steps.

3.1. The wall-cluster algorithm

Several variants of the cluster algorithm have been proposed in the literature. The best known are the (original) Swendsen–Wang algorithm [28] and the single-cluster algorithm of Wolff [29]. In all of these variants, the definition of a cluster is the same. Let us briefly recall this definition in the example of the Ising model. A link between two nearest-neighbour sites x and y is deleted with the probability

$$p_{\text{d}} = \min[1, \exp(-2\beta s_x s_y)] \tag{14}$$

where $s_x \in \{-1, 1\}$ is the spin at the site x. The links that are not deleted are frozen. A cluster is a set of sites that is connected by frozen links. The variants of the cluster algorithm differ by the selection of clusters that are flipped. To flip a cluster means to change the sign of the spins within the cluster. In the Swendsen–Wang algorithm all clusters are explicitly constructed, and a cluster is flipped with the probability of $1/2$. In Wolff's single-cluster algorithm, one site of the lattice is randomly selected. Only the cluster that contains this site is flipped. For this purpose, only this single cluster has to be constructed.

In the wall-cluster algorithm of [14] all clusters that intersect with an L^2 plane ('wall') of the lattice are flipped. Similar to the single-cluster algorithm, only those clusters that are flipped have to be constructed.

In [14], for the three-dimensional Ising model, a small gain in performance compared with the single-cluster algorithm was found. In addition, the wall-cluster update can be combined with the measurement of the ratio of partition functions Z_a/Z_p.

In order to apply the wall-cluster algorithm, or any other cluster algorithm, discussed above to the N-component ϕ^4 theory, Ising variables are embedded into the model. This idea goes back to Wolff [29]: in one step of the update, a unit vector $\vec{u}$ in $\mathbb{R}^N$ is selected. Only the sign of the component of the field parallel to this unit vector is allowed to change. That is, if we write $\phi_x^{(p)} := \vec{u} \cdot \vec{\phi}_x$ as

$$\phi_x^{(p)} = s_x |\phi_x^{(p)}| \tag{15}$$

where $s_x \in \{-1, 1\}$, only s_x might change in the update. Ignoring constant terms, we arrive at the action of the embedded Ising system:

$$S_{\text{embed}} = -\sum_{\langle xy \rangle} \beta_{\langle xy \rangle} s_x s_y \tag{16}$$

with $\beta_{\langle xy \rangle} = \beta |\phi_x^{(p)}||\phi_y^{(p)}|$. Using equation (14) we get

$$p_d = \min[1, \exp(-2\beta_{\langle xy \rangle} s_x s_y)] = \min[1, \exp(-2\beta \phi_x^{(p)} \phi_y^{(p)})] \tag{17}$$

for the N-component ϕ^4 model.

In [29], for each update step, $\vec{u}$ is randomly chosen with a uniform probability distribution. Here, we choose $\vec{u} = (1, 0, \ldots, 0), (0, 1, \ldots, 0), \ldots, (0, 0, \ldots, 1)$ in a fixed sequence. This simplifies the implementation of the cluster update and the measurement of Z_a/Z_p. Also CPU time is saved since in one update step only one component of the field has to be accessed. In order to compensate for this restricted choice of $\vec{u}$, we perform a global rotation of the field after a certain number of cluster updates, where the rotation matrix is randomly selected. Note that such a selection of $\vec{u}$ has already been used in [6, 30].

3.2. The local update of the ϕ^4 model

We sweep through the lattice in typewriter fashion with a local Metropolis update.

A proposal for a new field at the site x is generated by

$$\phi_x'^{(i)} = \phi_x^{(i)} + c\,(r^{(i)} - 0.5) \tag{18}$$

where $r^{(i)}$ are random numbers that are uniformly distributed in $[0, 1)$, i runs from 1 to N. The proposal is accepted with the probability

$$A = \min[1,\ \exp(-S' + S)] \tag{19}$$

where S' is the action of the proposed field ϕ' and S is the action of the original field. The step-size c is adjusted such that the acceptance rate is about $1/2$. After this Metropolis step, at the same site we perform an over-relaxation step:

$$\vec{\phi}_x' = \vec{\phi}_x - 2\,\frac{(\vec{\phi}_x \cdot \vec{\phi}_n)\,\vec{\phi}_n}{\vec{\phi}_n^2} \tag{20}$$

where $\vec{\phi}_n$ is the sum of nearest neighbours of $\vec{\phi}_x$. Note that this step takes very little CPU time; hence it is likely that its benefit outbalances the CPU cost. Due to a lack of time, we did not check this point carefully.

3.3. The update cycle

Above we have discussed the building blocks of our update. These building blocks are composed into a basic cycle:

- local update sweep (this step is omitted for the nonlinear σ models);
- global rotation of the field;
- $3 \times N$ wall-cluster updates.

The sequence of the $3 \times N$ wall-cluster updates is as follows. The wall is chosen in sequence to be perpendicular to the 1-, 2- and 3-directions of the lattice. Each time, the position of the wall is randomly selected. For each of the three directions of the wall, a wall-cluster update is performed for the N choices $(1, 0, \ldots, 0)$, $(0, 1, \ldots, 0)$, $\ldots$, $(0, 0, \ldots, 1)$ of $\vec{u}$.

4. The simulations

All our simulations were started with an ordered configuration. For equilibration, we discarded the configurations that were generated by the first 10^5 update cycles (see section 3.3). Note that $10^5 \gg \tau$, as we shall see below. After equilibration, we measured the observables after each update cycle. In order to reduce the amount of data that is written to disk, during the simulation we averaged the results of 5000 measurements. These averages were saved.

First we have simulated the $O(3)$-invariant nonlinear σ model at the best estimate of $\beta_c = 0.693\,002(12)$ of [9]. We used lattices of sizes $L = 6$, 8, 12, 16, 24, 32 and 48. We have performed 25×10^6 measurements for $L = 6$–32 and 10^7 measurements for $L = 48$.

The $N = 3$ ϕ^4 model was simulated at $\lambda = 2.0$, 4.5 and 5.0 on lattices of linear sizes $L = 6$, 8, 12, 16, 24 and 32. For $\lambda = 4.5$ we simulated in addition $L = 48$. In all cases we performed 10^7 measurements.

We have simulated the $O(4)$-invariant nonlinear σ model at the estimate of $\beta_c = 0.935\,861(8)$ of [9]. We studied lattices of sizes $L = 6$, 8, 12, 16, 24, 32 and 48. We have performed 25×10^6 measurements for $L = 6$–16, 2×10^7 measurements for $L = 24$, 14×10^6 measurements for $L = 32$, and 105×10^5 measurements for $L = 48$.

The $N = 4$ ϕ^4 model was simulated at $\lambda = 8.0$, 12.0 and 14.0 on lattices of the linear sizes $L = 6$, 8, 12, 16, 24 and 32. For $\lambda = 12.0$ we simulated in addition $L = 48$. As for $N = 3$, we performed 10^7 measurements for each parameter set.

In the case of the ϕ^4 model we have simulated at estimates of β_f from $Z_a/Z_{p,f}$, which were obtained from smaller lattice sizes that have been simulated before and/or short test-simulations.

For all our runs, we have determined the integrated auto-correlation time τ_{int} of the magnetic susceptibility χ and $\sum_{\langle xy \rangle} \vec{\phi}_x \cdot \vec{\phi}_y$. For example, for the $N = 3$ ϕ^4 model at $\lambda = 4.5$ we find that the integrated auto-correlation time of χ in units of cycles (see section 3.3) grows from $\tau_{int} = 2.1$ for $L = 6$ to about $\tau_{int} = 3.3$ for $L = 48$. The integrated auto-correlation time of $\sum_{\langle xy \rangle} \vec{\phi}_x \cdot \vec{\phi}_y$ is larger than that of χ. It grows from $\tau_{int} = 2.6$ for $L = 6$ to about $\tau_{int} = 5.1$ for $L = 48$. Note that in the preprint version of [17] a detailed discussion is presented of the auto-correlation times of the wall-cluster algorithm applied to the $N = 2$ ϕ^4 model.

As a random number generator we have used our own implementation of G05CAF of the NAG library. The G05CAF is a linear congruential random number generator with modulus $m = 2^{59}$, multiplier $a = 13^{13}$ and increment $c = 0$.

As a check of the correctness of the program and the quality of the random number generator we have implemented the following two non-trivial relations among observables:

$$0 = \tfrac{1}{2}\beta \sum_{y \cdot nn \cdot x} \langle \vec{\phi}_x \vec{\phi}_y \rangle \; - \; \langle \vec{\phi}_x^2 \rangle \; - \; 2\lambda \, \langle (\vec{\phi}_x^2 - 1)\, \vec{\phi}_x^2 \rangle \; + \; \tfrac{N}{2} \tag{21}$$

and

$$0 = \beta \left\langle \left(\sum_{y \cdot nn \cdot x} [\phi_x^1 \phi_y^2 - \phi_x^2 \phi_y^1] \right)^2 \right\rangle - \frac{2}{N} \sum_{y \cdot nn \cdot x} \langle \vec{\phi}_x \vec{\phi}_y \rangle \tag{22}$$

where $y \cdot nn \cdot x$ indicates that the sum runs over the six nearest neighbours of x. In order to enhance the statistics, we have summed equations (21) and (22) over all sites x. We found that for all our simulations these equations are satisfied within the expected statistical errors.

Most of the simulations were performed on 450 MHz Pentium III PCs. For our largest lattice size $L = 48$, one update cycle plus a measurement takes 0.67, 0.58, 0.86 and 0.75 s for the $N = 3$ ϕ^4 model at $\lambda = 4.5$, $\beta = 0.686\,22$, the $O(3)$-invariant nonlinear σ model at $\beta = 0.693\,002$, the $N = 4$ ϕ^4 model at $\lambda = 12.0$, $\beta = 0.908\,43$ and the $O(4)$-invariant nonlinear σ model at $\beta = 0.935\,861$, respectively.

In total, the whole study took about two years on a single 450 MHz Pentium III CPU.

5. Analysis of the data

In our analysis the observables are needed as a function of β. Given the large statistics we did not use the reweighting technique. Instead we used the Taylor expansion up to the third order. The coefficients were obtained from the simulation. We have always checked that β_f are sufficiently close to β of the simulation such that the error from the truncation of the Taylor series is well below the statistical error. Statistical errors are computed by a Jackknife analysis.

5.1. Corrections to scaling

In the first step of the analysis we have estimated ξ_{2nd}/L^* and Z_a/Z_p^* by fitting the $O(3)$- and $O(4)$-invariant nonlinear σ model data with the ansatz

$$R(\beta_c) = R^* + c\, L^{-\omega} \tag{23}$$

where β_c, R^* and c are the parameters of the fit. We have fixed $\omega = 0.8$. As result we have obtained $Z_a/Z_p^* \approx 0.196$ and $\xi_{2nd}/L \approx 0.564$ for the $O(3)$ model and $Z_a/Z_p^* \approx 0.1195$ and $\xi_{2nd}/L^* \approx 0.547$ for the $O(4)$ model. In the following we shall use these numbers to set $R_{1,f}$: i.e. $Z_a/Z_{p,f} = 0.196$ and $\xi_{2nd}/L_f = 0.564$ for $N = 3$ and $Z_a/Z_{p,f} = 0.1195$ and $\xi_{2nd}/L_f = 0.547$ for $N = 4$.

Next we have analysed $\bar{R}$ to study corrections to scaling. To obtain a first impression, we have plotted our results for $\bar{R}$ with $Z_a/Z_{p,f}$ for $N = 3$ in figure 1 and for $N = 4$ in figure 2. In both cases the range $6 \leqslant L \leqslant 32$ is shown.

Let us discuss the $N = 3$ case in detail. For the $O(3)$-symmetric nonlinear σ model, we clearly see an increase of $\bar{R}$ with increasing L over the whole range of lattice sizes. On the other side, for $\lambda = 2.0$, $\bar{R}$ decreases. For $\lambda = 4.5$ and 5.0 $\bar{R}$ remains almost constant. This behaviour suggests that leading corrections to scaling vanish at $\lambda^* \approx 5$. The behaviour of $\bar{R}$ for $N = 4$ is qualitatively the same as for $N = 3$. Figure 2 indicates that $\lambda^* \approx 13$.

In the following numerical analysis of the data we demonstrate that the behaviour discussed above is indeed due to leading corrections to scaling, and we give an accurate estimate of λ^* and its error bar. For this purpose we fitted our data for $\bar{R}$ with the ansatz

$$\bar{R} = \bar{R}^* + \bar{c}(\lambda)\, L^{-\omega} \tag{24}$$

with $\bar{R}^*$, $\bar{c}(\lambda)$ for each value of λ and ω as free parameters. For $N = 3$ and 4, we have performed such fits for three different sets of input data. These sets are given in table 1.

Our results for $\bar{R}^*$ and ω for $N = 3$ are given in table 2.

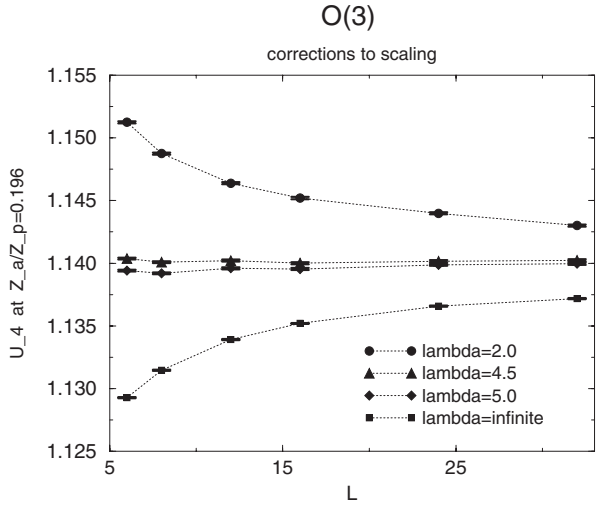

Figure 1. $N = 3$. The Binder cumulant U at $Z_a/Z_{p,f} = 0.196$ as a function of the lattice size L for $\lambda = 2.0$, 4.5, 5.0 and ∞. The dotted curve is drawn only as a guide to the eye.

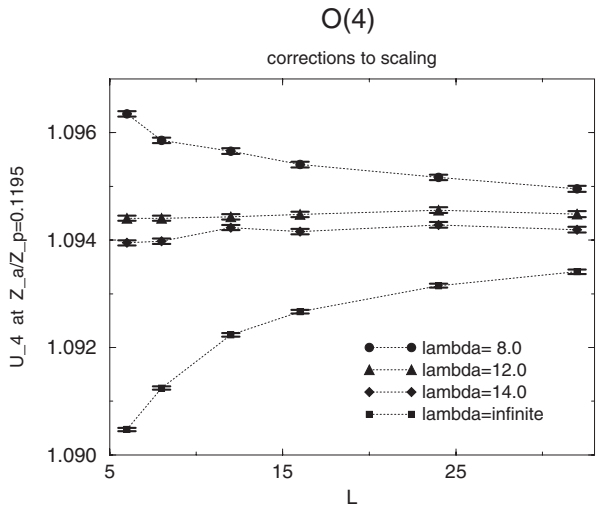

Figure 2. $N = 4$. The Binder cumulant U at $Z_a/Z_{p,f} = 0.1195$ as a function of the lattice size L for $\lambda = 8.0$, 12.0, 14.0 and ∞. The dotted curve is drawn only as a guide to the eye.

The values of $\bar{c}$ from the same fits are summarized in table 3. First of all, we notice that the results of our fit for ω are consistent with the estimates from field-theoretic methods (see table 9). Given the statistical error and the variation of our result for ω with the different data sets, we cannot provide a more accurate estimate for ω than the field-theoretic methods.

Having convinced ourselves that we really see leading corrections to scaling, we extract an estimate for λ^* from the data given in table 3. Therefore, we linearly extrapolate the results of $\bar{c}$ at $\lambda = 4.5$ and 5.0. Taking the results from set 1 we arrive at the estimate $\lambda^* = 4.4(7)$, where the results from U_4 at $Z_a/Z_{p,f}$ and U_4 at ξ_{2nd}/L_f are consistent. The error bar is computed from the variation of λ^* with the data sets used for the fit. For U_4 at $Z_a/Z_{p,f}$, λ^* is roughly the same for all

Table 1. The sets of input data for fits with equation (24). For $N = 3$ as well as 4 we have fitted three different sets of input data. In columns one and two, the λ-values for $N = 3$ and 4 are given, respectively. In columns three, four and five, the lattice sizes L that have been included in the fits are listed.

λ, $N = 3$	λ, $N = 4$	Set 1	Set 2	Set 3
2.0	8.0	16, 24, 32	12, 16, 24	8, 12, 16
4.5	12.0	16, 24, 32, 48	12, 16, 24, 32	8, 12, 16, 24
5.0	14.0	16, 24, 32	12, 16, 24	8, 12, 16
∞	∞	16, 24, 32, 48	12, 16, 24, 32	8, 12, 16, 24

Table 2. Results for $\bar{R}^*$ and ω for $N = 3$ from fits with the ansatz (24). The data sets that have been used for the fits are given in table 1. The results for $\bar{c}$ from the same fits are summarized in table 3.

Set	χ^2/d.o.f.	$\bar{R}^*$	ω
		U_4 at $Z_a/Z_{p,f}$	
1	2.32	1.140 18(9)	0.743(23)
2	1.79	1.140 28(9)	0.749(18)
3	1.14	1.140 21(8)	0.799(13)
		U_4 at ξ_{2nd}/L	
1	2.16	1.139 77(10)	0.741(22)
2	0.90	1.140 00(11)	0.732(17)
3	4.06	1.140 38(10)	0.775(12)

Table 3. Results for $\bar{c}$ for $N = 3$ from fits with the ansatz (24). The results for $\bar{R}^*$ and ω are given in table 2.

Set	$\bar{c}(2.0)$	$\bar{c}(4.5)$	$\bar{c}(5.0)$	$\bar{c}(\infty)$
		U_4 at $Z_a/Z_{p,f}$		
1	0.0392(33)	–0.0008(10)	–0.0042(8)	–0.0390(24)
2	0.0394(25)	–0.0011(8)	–0.0049(7)	–0.0408(17)
3	0.0451(17)	–0.0007(6)	–0.0053(5)	–0.0461(11)
		U_4 at ξ_{2nd}/L_f		
1	0.0464(37)	–0.0007(11)	–0.0056(9)	–0.0464(26)
2	0.0436(27)	–0.0026(8)	–0.0074(7)	–0.0475(18)
3	0.0452(18)	–0.0064(6)	–0.0115(5)	–0.0566(12)

three sets. However, for U_4 at ξ_{2nd}/L_f, there is a drift to larger results for λ^* as the lattice sizes increase. Assuming a convergence proportional $L^{-\omega'+\omega} \approx L^{-0.8}$ we arrive at our error estimate.

In tables 4 and 5 we have summarized our results for $\bar{R}^*$ and ω and $\bar{c}$ for $N = 4$. As for $N = 3$, we see that the values for ω are consistent with the field-theoretic results.

Clearly, the sign of $\bar{c}(\infty)$ is negative and that of $\bar{c}(8.0)$ is positive. Hence a λ^* exists with $\bar{c}(\lambda^*) = 0$. From linear interpolation of the result for $\lambda = 12.0$ and 14.0 we arrive at $\lambda^* = 12.5(4.0)$. The error bar has been computed in the same way as for $N = 3$.

We have also used a slightly different approach to compute ω from the available data. We have analysed the difference of $\bar{R}$ at $\lambda = 2.0$ and $\lambda = \infty$. Obviously, $\bar{R}^*$ is cancelled in this way. Also, one might expect that corrections which are quadratic in the leading corrections cancel since $|\bar{c}(2.0)|$ and $|\bar{c}(\infty)|$ are almost the same. In addition, the analysis of numerical data for $N = 1$ in [15] and $N = 2$ in [16] suggests that sub-leading corrections also cancel to

Table 4. Results for $\bar{R}^*$ and ω for $N = 4$ from fits with the ansatz (24). The data sets that have been used for the fits are given in table 1. The results for $\bar{c}$ from the same fits are summarized in table 5.

Set	χ^2/d.o.f.	$\bar{R}^*$	ω
		U_4 at $Z_a/Z_{p,f}$	
1	0.75	1.094 41(6)	0.798(52)
2	0.84	1.094 50(7)	0.748(41)
3	2.07	1.094 66(6)	0.761(27)
		U_4 at ξ_{2nd}/L	
1	0.77	1.094 58(7)	0.761(50)
2	1.08	1.094 74(8)	0.735(37)
3	7.51	1.095 22(8)	0.761(25)

Table 5. Results for $\bar{c}$ for $N = 4$ from fits with the ansatz (24). The results for $\bar{R}^*$ and ω are given in table 4.

Set	$\bar{c}(8.0)$	$\bar{c}(12.0)$	$\bar{c}(14.0)$	$\bar{c}(\infty)$
		U_4 at $Z_a/Z_{p,f}$		
1	0.0091(19)	0.0010(8)	−0.0023(7)	−0.0160(22)
2	0.0073(12)	−0.0001(6)	−0.0021(5)	−0.0145(14)
3	0.0061(7)	−0.0013(4)	−0.0033(3)	−0.0165(8)
		U_4 at ξ_{2nd}/L_f		
1	0.0083(18)	0.0011(8)	−0.0035(6)	−0.0183(23)
2	0.0065(12)	−0.0017(6)	−0.0040(5)	−0.0184(15)
3	0.0030(7)	−0.0059(4)	−0.0080(3)	−0.0239(10)

Table 6. Results for ω for $N = 3$ and 4 obtained by fitting with ansatz (25). In the first column we give N and the dimensionless ratio that has been used to determine β_f. In the fit all lattice sizes with $L_{min} \leqslant L \leqslant L_{max}$ have been taken into account.

	L_{min}	L_{max}	χ^2/d.o.f.	ω
$N = 3$, U_4 at $Z_a/Z_p = 0.196$	6	32	1.67	0.796(7)
	8	32	0.73	0.781(10)
$N = 3$, U_4 at $\xi_2/L = 0.564$	6	32	0.65	0.769(6)
	8	32	0.65	0.766(9)
$N = 4$, U_4 at $Z_a/Z_p = 0.1195$	6	32	0.54	0.780(15)
	8	32	0.40	0.765(22)
$N = 4$, U_4 at $\xi_2/L = 0.547$	6	32	0.40	0.774(14)
	8	32	0.38	0.764(20)

a large extent. Therefore, we have fitted our data with the ansatz

$$\bar{R}(L, \lambda)|_{\lambda=2.0} - \bar{R}(L, \lambda)|_{\lambda=\infty} = \Delta\bar{c}\, L^{-\omega}. \tag{25}$$

Our results for $N = 3$ and the corresponding results for $N = 4$ are given in table 6. In the case of $N = 4$ we have taken the difference of $\bar{R}$ at $\lambda = 8.0$ and $\lambda = \infty$.

First we notice that χ^2/d.o.f. ≈ 1 is already reached for $L_{min} = 6$. For such a small L_{min}, fits with ansatz (24) produce χ^2/d.o.f. $= 2.8$ for $N = 3$, U_4 at $Z_a/Z_p = 0.196$ and χ^2/d.o.f. $= 13.3$ for $N = 3$, U_4 at $\xi_2/L = 0.564$. This fact indicates that the above-mentioned cancellations indeed occur.

Table 7. Results for ν from fits with the ansatz (26). The range of lattice sizes is always $L_{\min} = 16$ and $L_{\max} = 32$. We have used six different combinations of R. These are given by: C1, the slope of U_4 at $Z_a/Z_{p,f}$; C2, the slope of Z_a/Z_p at $Z_a/Z_{p,f}$; C3, the slope of ξ_{2nd}/L at $Z_a/Z_{p,f}$; C4, the slope of U_4 at ξ_{2nd}/L_f; C5, the slope of Z_a/Z_p at ξ_{2nd}/L_f; C6, the slope of ξ_{2nd}/L at ξ_{2nd}/L_f.

λ	C1	C2	C3	C4	C5	C6
2.0	0.7164(23)	0.7088(10)	0.7136(13)	0.7181(24)	0.7106(12)	0.7135(12)
4.5	0.7071(21)	0.7083(9)	0.7115(12)	0.7074(21)	0.7086(10)	0.7115(12)
5.0	0.7078(21)	0.7085(9)	0.7114(11)	0.7071(21)	0.7077(10)	0.7114(11)
∞	0.7076(12)	0.7127(5)	0.7142(6)	0.7056(12)	0.7136(13)	0.7141(6)

The results for ω are consistent with those of the field-theoretic methods. Certainly our approach is very promising to give competitive results for the correction exponent ω. However, we would like to have still larger statistics and a larger range of lattice sizes to give a sensible estimate of the systematic error caused by sub-leading corrections.

5.2. Critical exponents

We have computed the critical exponents ν and η using well-established finite-size scaling methods. Below we shall only discuss in detail the results for $N = 3$. The analysis for $N = 4$ has been performed analogously.

The exponent ν is computed from the slope of a dimensionless ratio R at β_f (see equation (11)):

$$\left.\frac{\partial R}{\partial \beta}\right|_{\beta_f} = a\, L^{1/\nu}. \tag{26}$$

As was pointed out in [9], replacing β_c by β_f simplifies the error analysis, since the error in β_c does not need to be propagated.

In our study we have considered three different choices of R. Hence, in equation (26) we could in principle consider nine different combinations. Below we shall restrict ourselves to six choices: β_f is fixed either by $Z_a/Z_{p,f}$ or ξ_{2nd}/L_f. We consider the slope of all three dimensionless ratios R.

First we would like to study how much the result of ν from fits with equation (26) depends on leading corrections to scaling. For this purpose, for $L_{\min} = 16$ and $L_{\max} = 32$, we have fitted our data for all available values of λ for all six combinations of R. The results of these fits are summarized in table 7.

The variation of the results with λ are rather small. We find the largest variation for the combination C1, where we obtain $\nu = 0.7164(23)$ for $\lambda = 2.0$ and $\nu = 0.7076(12)$ for $\lambda = \infty$. Hence, we expect that for $\lambda = 4.5$ the effect of corrections to scaling should be smaller than 0.0001.

Next, let us discuss in more detail the results for $\lambda = 4.5$ which is closest to our estimate of λ^*. The results from fits with ansatz (26) are summarized in table 8. We see that the results approach each other as $L_{\min}$ is increased. For the slope of U_4, the results for ν remain almost constant as $L_{\min}$ is varied. For the slope of Z_a/Z_p we see a slight increase of the estimate of ν. On the other hand, for the slope of ξ_{2nd}/L, we see a decrease. Assuming that this behaviour is caused by the sub-leading corrections, we conclude that $\nu = 0.7120$ from ξ_{2nd}/L is an upper bound. Given the larger stability of the estimate from Z_a/Z_p, we take $\nu = 0.710(2)$ as our final estimate.

Table 8. Results for ν from fits with ansatz (26) for $N = 3$ at $\lambda = 4.5$; always $L_{\max} = 48$. The combinations C1, ..., C6 are explained in the caption of table 7.

$L_{\min}$	C1	C2	C3	C4	C5	C6
8	0.7113(7)	0.7087(3)	0.7150(4)	0.7102(7)	0.7075(3)	0.7150(4)
12	0.7111(10)	0.7100(4)	0.7132(5)	0.7107(10)	0.7096(5)	0.7132(5)
16	0.7101(13)	0.7099(6)	0.7120(7)	0.7102(14)	0.7100(7)	0.7120(7)

Table 9. Results for the critical exponents of the $O(3)$ universality class from various methods.

Method	Reference	ν	η	ω
IMC	Present work	0.710(2)	0.0380(10)	0.773
MC	[9]	0.7128(14)	0.0413(15)(1)	0.78(2)
MC	[8]	0.642(2)	0.020(1)	—
MC	[7]	0.704(6)	0.027(2)	—
MC	[5]	0.704(6)	0.028(2)	—
MC	[4]	0.706(9)	0.031(7)	—
MC	[6]	0.7036(23)	0.0250(35)	—
HT	[31]	0.715(3)	0.036(10)[a]	—
$d = 3$ PT	[12]	0.7073(35)	0.0355(25)	0.782(13)
ϵ-expansion	[12]	0.7045(55)	0.0375(45)	0.794(18)

[a] This number for η is computed from $\gamma = 1.404(4)$ and $\nu = 0.715(3)$ given in the reference; the details are discussed in the text.

Next we compute the exponent η from the finite-size behaviour of the magnetic susceptibility

$$\chi|_{\beta_f} = c\, L^{2-\eta}. \tag{27}$$

We restrict the discussion to $Z_a/Z_{p,f}$ since fixing β_f by ξ_{2nd}/L_f gives very similar numbers.

For the estimate of η we see a much stronger dependence on λ than for ν. Fitting with ansatz (27) and $L_{\min} = 16$, $L_{\max} = 32$ we obtain $\eta = 0.039\,82(33)$, $0.036\,14(30)$, $0.035\,41(31)$ and $0.032\,69(18)$ for $\lambda = 2.0$, 4.5, 5.0 and ∞, respectively.

Fitting the data at $\lambda = 4.5$ with $L_{\max} = 48$ yields $\eta = 0.035\,81(14)$, $0.036\,68(19)$ and $0.037\,36(32)$ for $L_{\min} = 12$, 16 and 24, respectively. For $L_{\min} = 12$ we get $\chi^2/\text{d.o.f.} = 18.5$. The strong dependence of the result on $L_{\min}$ and the large $\chi^2/\text{d.o.f.}$ at $L_{\min} = 12$ indicates that there are sizeable sub-leading corrections.

Fitting with an ansatz that includes an analytic background term

$$\chi|_{\beta_f} = c\, L^{2-\eta} + b \tag{28}$$

yields $\chi^2/\text{d.o.f.} = 0.38$ already for $L_{\min} = 8$. The results are $\eta = 0.0384(2)$, $0.0386(4)$ and $0.0381(6)$ for $L_{\min} = 8$, 12 and 16, respectively. To see the effect of leading corrections on this fit we have in addition fitted the data for $\lambda = 5.0$ with $L_{\min} = 8$ and $L_{\max} = 32$; we get $\eta = 0.0378(4)$.

As our final estimate we quote $\eta = 0.0380(10)$. The error bar takes into account statistical errors as well systematic errors due to leading and sub-leading corrections. These errors are estimated from the spread of the results of the various fits discussed above.

With a similar analysis we arrive at $\nu = 0.749(2)$ and $\eta = 0.0365(10)$ for the $O(4)$ universality class.

Table 10. Results for the critical exponents of the $O(4)$ universality class from various methods.

Method	Reference	ν	η	ω
IMC	Present work	0.749(2)	0.0365(10)	0.765
MC	[11]	0.739(2)[a]	0.024(2)[a]	—
MC	[9]	0.7525(10)	0.0384(12)	1.8(2)
MC	[10]	0.7479(90)	0.0254(38)	—
HT	[31]	0.750(3)	0.035(9)[b]	—
$d = 3$ PT	[12]	0.741(6)	0.0350(45)	0.774(20)
ϵ-expansion	[12]	0.737(8)	0.0360(40)	0.795(30)

[a] These numbers for ν and η are computed from $\delta = 4.86(1)$ and $\beta = 0.3785(6)$ that are given in the reference; the details are discussed in the text.
[b] This number for η is computed from $\gamma = 1.474(4)$ and $\nu = 0.750(3)$ that are given in the reference; the details are discussed in the text.

6. Comparison with results from the literature

Here we would like to compare our results for the critical exponents ν and η with previous Monte Carlo studies of the $O(3)$- and $O(4)$-invariant nonlinear σ models. In addition we give selected results from high-temperature series, perturbation theory in three dimensions, and the ϵ-expansion. The results are summarized in tables 9 and 10 for $N = 3$ and 4, respectively. For more references on field-theoretic methods and other methods not discussed here, see for example [12].

All Monte Carlo studies listed in tables 9 and 10 use a simple cubic lattice. In addition, in [6] the body centred cubic lattice is studied. (In table 9 we only give the simple cubic results.) All studies except [11] use finite-size scaling to determine critical exponents. In all finite-size scaling studies, the lattice sizes are smaller or equal to $L = 48$, except for [9], where in addition $L = 64$ is simulated. The results of the Monte Carlo (MC) studies cited above are extracted from ansatz-like equations (26) and (27) (mostly β_c is used instead of β_f). We see that almost all Monte Carlo results for ν are consistent with ours. On the other hand, the results for η are systematically too small, except for [9].

This behaviour can be well understood with our results of section 5.2. The estimates for η from the ansatz (27) are clearly affected by corrections to scaling. Our results from the $O(3)$- and $O(4)$-invariant nonlinear σ models for η are systematically lower than our final results from the ϕ^4 models at λ^*. On the other hand, the results for ν given in table 7 show only little variation with λ; i.e. little dependence on leading corrections to scaling.

The authors of [9], who for the first time tried to take into account leading corrections to scaling in the analysis of their data, arrive at rather similar conclusions as to how leading corrections to scaling affect the estimates of η and ν. They extrapolated their results for η assuming $L^{-\omega}$ corrections.

However from our analysis of section 5.2 we know that the estimates of η obtained from lattices with $L \leqslant 48$ are also strongly affected by sub-leading corrections with $\omega' \approx 2$.

Hence, extrapolating only in $L^{-\omega}$ leads to a wrong amplitude for the $L^{-\omega}$ corrections. As a result, the final estimate of [9] for η is too large compared with our result.

The authors of [11] determine on lattices of a size up to 120^3 the magnetization m in the thermodynamic limit. They estimate the critical exponents β and δ by fitting their data with the ansatz

$$m(t, 0) \sim t^{\beta} \qquad m(0, h) \sim h^{1/\delta}. \tag{29}$$

We have converted their results by using the scaling relations $\nu = \beta/(d - y_h)$ and $\eta = d + 2 - 2y_h$, where $y_h = \delta d/(1 + \delta)$ and $d = 3$ is the dimension. As one can see

from table 10 there is a clear discrepancy with our numbers for η as well as ν; i.e. ignoring corrections to scaling in equations (29) leads to similar problems as in finite-size scaling.

There are a large number of references on the ϵ-expansion and the perturbative expansion in three dimensions in the literature. As an example, we have chosen the result of a recent analysis by Guida and Zinn-Justin [12]. We notice that these results are consistent with ours for η and ν within the quoted errors. Also, we note that the error bars of our estimates for ν and η are smaller than those of the field-theoretic estimates.

There are also a number of publications on the analysis of high-temperature series. In the tables we give the results of a recent analysis [31] using inhomogeneous differential approximants. The coefficients of the high-temperature series of χ and μ_2 are computed up to β^{21}. In our tables, we only give the results from the unbiased analysis of the simple cubic lattice series. In addition, the authors analyse the body centred cubic lattice. The authors also give results obtained from a so-called θ-biased analysis, where they make use of the numerical results for $\theta = \omega\nu$ obtained from field-theoretic methods. It is interesting to note that these biased results (not given in our tables) tend to be less consistent with our results than the unbiased results which we quote in tables 9 and 10.

In tables 9 and 10, for ω we give the average of the result from $Z_a/Z_{p,f}$ and ξ_{2nd}/L_f with $L_{min} = 8$ taken from table 6. We make no attempt to estimate the systematic errors due to subleading corrections. Certainly these errors are larger than those quoted for the field-theoretic estimates of [12]. It is however interesting to note that our results are consistent with those of [12].

Also, the Monte Carlo result of [9] for $N = 3$ is consistent with ours. However we cannot confirm their surprising result for $N = 4$.

7. Conclusions

In this study we have demonstrated that the program of [13,14] to eliminate leading corrections to scaling in the three-dimensional ϕ^4 model can be extended to $N = 3$ and 4. In particular, we have found $\lambda^* = 4.4(7)$ for $N = 3$ and $\lambda^* = 12.5(4.0)$ for $N = 4$. Based on these results, we have computed the critical exponents ν and η from finite-size scaling. In particular, for η, the error bar could be reduced considerably compared with previous Monte Carlo simulations or field-theoretic methods and the analysis of high-temperature series.

Since the CPU time used for the present study is still moderate, further progress can be made just by enlarging the statistics and simulating larger lattices.

Also, our results for λ^* can be used as input for the analysis of high-temperature series analogous to [18, 19].

The principal question raised in [18], whether the program to eliminate leading corrections is restricted to $N < N_c$, where N_c is finite, remains open.

Acknowledgments

I would like to thank M Campostrini, A Pelissetto, P Rossi and E Vicari for discussions and comments on the manuscript. I would also like to thank M Müller-Preußker for giving me access to the PC-pool of his group.

References

[1] Wilson K G and Kogut J 1974 *Phys. Rep.* C **12** 75
[2] Cardy J 1996 *Scaling and Renormalization in Statistical Physics* (Cambridge: Cambridge University Press)

[3] Domb C 1996 *The Critical Point, A Historical Introduction to the Modern Theory of Critical Phenomena* (London: Taylor and Francis)
[4] Peczak P, Ferrenberg A M and Landau D P 1991 *Phys. Rev.* B **43** 6087
[5] Holm C and Janke W 1993 *Phys. Lett.* A **173** 8
(Holm C and Janke W 1992 *Preprint* hep-lat/9209017)
[6] Chen K, Ferrenberg A M and Landau D P 1993 *Phys. Rev.* B **48** 3249
[7] Holm C and Janke W 1993 *Phys. Rev.* B **48** 936
(Holm C and Janke W 1993 *Preprint* hep-lat/9301002)
[8] Brown R G and Ciftan M 1996 *Phys. Rev. Lett.* **76** 1352
[9] Ballesteros H G, Fernandez L A, Martin-Mayor V and Munoz-Sudupe A 1996 *Phys. Lett.* B **387** 125
(Ballesteros H G, Fernandez L A, Martin-Mayor V and Munoz-Sudupe A 1996 *Preprint* cond-mat/9606203)
[10] Kanaya K and Kaya S 1995 *Phys. Rev.* D **51** 2404
[11] Engels J and Mendes T 2000 *Nucl. Phys.* B **572** 289
(Engels J and Mendes T 1999 *Preprint* hep-lat/9911028)
[12] Guida R and Zinn-Justin J 1998 *J. Phys. A: Math. Gen.* **31** 8103
(Guida R and Zinn-Justin J 1998 *Preprint* cond-mat/9803240)
[13] Ballesteros H G, Fernandez L A, Martin-Mayor V and Munoz-Sudupe A 1998 *Phys. Lett.* B **441** 330
(Ballesteros H G, Fernandez L A, Martin-Mayor V and Munoz-Sudupe A 1998 *Preprint* hep-lat/9805022)
[14] Hasenbusch M, Pinn K and Vinti S 1999 *Phys. Rev.* B **59** 11 471
(Hasenbusch M, Pinn K and Vinti S 1998 *Preprint* hep-lat/9806012)
(Hasenbusch M, Pinn K and Vinti S 1998 *Preprint* cond-mat/9804186 (unpublished))
[15] Hasenbusch M 1999 *J. Phys. A: Math. Gen.* **32** 4851
(Hasenbusch M 1999 *Preprint* hep-lat/9902026)
[16] Hasenbusch M and Török T 1999 *J. Phys. A: Math. Gen.* **32** 6361
(Hasenbusch M and Török T 1999 *Preprint* cond-mat/9904408)
[17] Campostrini M, Hasenbusch M, Pelissetto A, Rossi P and Vicari E 2001 *Phys. Rev.* B **63** 214503
(Campostrini M, Hasenbusch M, Pelissetto A, Rossi P and Vicari E 2000 *Preprint* cond-mat/0010360)
[18] Campostrini M, Pelissetto A, Rossi P and Vicari E 1999 *Phys. Rev.* E **60** 3526
(Campostrini M, Pelissetto A, Rossi P and Vicari E 1999 *Preprint* cond-mat/9905078)
[19] Campostrini M, Pelissetto A, Rossi P and Vicari E 2000 *Phys. Rev.* B **61** 5905
(Campostrini M, Pelissetto A, Rossi P and Vicari E 1999 *Preprint* cond-mat/9905395)
Campostrini M, Pelissetto A, Rossi P and Vicari E 2000 *Phys. Rev.* B **62** 5843
(Campostrini M, Pelissetto A, Rossi P and Vicari E 2000 *Preprint* cond-mat/0001440)
[20] Butera P and Comi M 1998 *Phys. Rev.* B **58** 11 552
(Butera P and Comi M 1998 *Preprint* hep-lat/9805025)
[21] Nightingale M P 1976 *Physica* A **83** 561
[22] Binder K 1981 *Z. Phys.* B **43** 119
Binder K 1981 *Phys. Rev. Lett.* **47** 693
[23] Hasenbusch M 1993 *J. Physique* **3** 753
(Hasenbusch M 1992 *Preprint* hep-lat/9209016)
[24] Gottlob A P and Hasenbusch M 1994 *J. Stat. Phys.* **77** 919
(Gottlob A P and Hasenbusch M 1994 *Preprint* cond-mat/9406092)
[25] Newman K E and Riedel E K 1984 *Phys. Rev.* B **30** 6615
[26] Campostrini M, Pelissetto A, Rossi P and Vicari E 1998 *Phys. Rev.* E **57** 184
[27] Brower R C and Tamayo P 1989 *Phys. Rev. Lett.* **62** 1087
[28] Swendsen R H and Wang J-S 1987 *Phys. Rev. Lett.* **58** 86
[29] Wolff U 1989 *Phys. Rev. Lett.* **62** 361
[30] Niedermayer F 1990 *Phys. Lett.* B **237** 473
[31] Butera P and Comi M 1997 *Phys. Rev.* B **56** 8212